Nonlinear Analysis: Modelling and Control, Vol. 31, No. 3, 699–721
https://doi.org/10.15388/namc.2026.31.46613

Vilnius University Press

On the dynamics of the autonomous Duffing–Holmes oscillator*

Érika Diz-Pita, Jaume Llibre, M. Victoria Otero-Espinar

Universidade de Santiago de Compostela,
Universitat Autónoma de Barcelona
erikadiz.pita@usc.es

Received: November 3, 2025 / **Revised:** March 9, 2026 / **Published online:** May 1, 2026

Abstract. The autonomous Duffing–Holmes oscillator $\dot{x} = y$, $\dot{y} = x - x^3 + by - kz$, $\dot{z} = w(y - z)$, depending on the three parameters b, k, and w, has been studied previously by several authors who showed that for certain parameter values, it exhibits chaotic motion, or that numerically it has two periodic orbits coming from a Hopf bifurcation, or that it can have three equilibria for some given values of the parameters. Here we provide new results on the integrability and the global dynamics of the autonomous Duffing–Holmes oscillator using its first integrals and Darboux invariants when these exist for some given values of its parameters.

Keywords: Duffing–Holmes model, first integral, rational first integral, invariant algebraic surface, Darboux invariant.

1 Introduction and statements of the main results

One of the most representative nonlinear differential systems exhibiting chaotic dynamics is the nonautonomous Duffing–Holmes oscillator. It is described by a second-order differential equation with an externally applied periodic driving term:

$$\ddot{x} + b\dot{x} - x + x^3 = a\sin(wt).$$

In [7], as an alternative to the nonautonomous Duffing–Holmes oscillator, the authors propose an autonomous version, defined as follows:

$$\dot{x} = y, \qquad \dot{y} = x - x^3 + by - kz, \qquad \dot{z} = w(y - z), \tag{1}$$

where $(x, y, z) \in \mathbb{R}^3$, and b, k, w are real parameters. Additionally, the authors developed a specialized electrical circuit to replicate the solutions of oscillator (1). The circuit was evaluated both numerically and experimentally, showing good agreement between simulation and physical results. The model can exhibit chaotic behavior.

*This research was supported by grants Nos. PID2020-115155GB-I00, ED431C 2023/31, and PID2022-136613NB-100.

In [6], the authors analyzed the differential system (1) for the specific values of the parameters $b = 1.9$, $k = 2.5$, and $w \in (2.5, 3.85)$. Under these conditions, system (1) has exactly three equilibrium points. They investigated the behavior of these equilibrium points depending on the parameter w, obtaining numerical results indicating that for $w \leqslant 3.55$, the three equilibrium points are nonattractive. Moreover, periodic orbits exist around two of them. When the parameter w decreases, the attracting properties of these two points weaken, and eventually, trajectories begin to move between the lateral equilibrium points, exhibiting irregular behavior and sensitivity to initial conditions. Later, the authors applied these observations to the study of some models in genetic network theory.

In [2], the authors prove the numerical results obtained in [6] by applying Hopf bifurcation theory, which provides the existence of two limit cycles around each equilibrium point, and show that, for the parameter values $b = 1.9$ and $k = 2.5$, the differential system (1) undergoes a Hopf bifurcation at $w = 3.64$.

In this paper, we give some results about the integrability and the global dynamics of the Duffing–Holmes model, given by the three-parameter family of systems (1), where b, k, and w are real parameters.

One can easily check that systems (1) are invariant under the change of variables

$$(x, y, z) \to (-x, -y, -z).$$

Consequently, if $(x(t), y(t), z(t))$ is a solution of systems (1), then $(-x(t), -y(t), -z(t))$ is also a solution.

Let $F = F(x, y, z) \in \mathbb{R}[x, y, z]$, where $\mathbb{R}[x, y, z]$ is the ring of real polynomials in the variables x, y, and z. The function F defines an *invariant algebraic surface* of system (1), $F = F(x, y, z) = 0$, if it satisfies the following condition:

$$\frac{\partial F}{\partial x}y + \frac{\partial F}{\partial y}\big(x - x^3 + by - kz\big) + \frac{\partial F}{\partial z}w(y - z) = KF,$$

where $K = K(x, y, z)$ is a real polynomial of degree at most 2, called the *cofactor* of $F(x, y, z)$. The following proposition provides a complete classification of all invariant algebraic surfaces of degree at most four of systems (1).

Proposition 1. *All the invariant algebraic surfaces of degree at most four of systems* (1) *for all values of the parameters are given in Table* 1.

Table 1. Invariant algebraic surfaces of systems (1), $F_i = F_i(x, y, z) = 0$ for $1 \leqslant i \leqslant 6$.

Conditions	$F_i = 0$	Cofactor
$b = 0, k = 0$	$F_1 = 2x^2 - x^4 - 2y^2$	$K_1 = 0$
$w = 0$	$F_2 = z$	$K_2 = 0$
$b = -w = -\frac{3}{\sqrt{22}}, k = -\frac{4}{\sqrt{22}}$	$F_3 = \sqrt{22}x^2 - \sqrt{22}x^4 - 4xy - 2\sqrt{22}y^2 + 16xz$	$K_3 = -4\sqrt{\frac{1}{22}}$
$b = -w = \frac{3}{\sqrt{22}}, k = \frac{4}{\sqrt{22}}$	$F_4 = \sqrt{22}x^2 - \sqrt{22}x^4 + 4xy - 2\sqrt{22}y^2 - 16xz$	$K_4 = 4\sqrt{\frac{1}{22}}$
$b = -\sqrt{\frac{3}{2}}, k = -2\sqrt{\frac{2}{3}}, w = \sqrt{\frac{2}{3}}$	$F_5 = \sqrt{6}x^2 - \sqrt{6}x^4 - 4xy - 2\sqrt{6}y^2 + 8xz + 2\sqrt{6}z^2$	$K_5 = -2\sqrt{\frac{2}{3}}$
$b = \sqrt{\frac{3}{2}}, k = 2\sqrt{\frac{2}{3}}, w = -\sqrt{\frac{2}{3}}$	$F_6 = \sqrt{6}x^2 - \sqrt{6}x^4 + 4xy - 2\sqrt{6}y^2 - 8xz + 2\sqrt{6}z^2$	$K_6 = 2\sqrt{\frac{2}{3}}$

Proof. We assume that $F(x,y,z)=0$ is an invariant algebraic surface of degree at most four for systems (1) and that $K=K(x,y,z)$ is its associated cofactor. Then

$$F(x,y,z)=\sum_{\substack{i,j,l\geqslant 0\\ i+j+l\leqslant 4}} a_{ijl}x^iy^jz^l \quad \text{and} \quad K(x,y,z)=\sum_{\substack{i,j,l\geqslant 0\\ i+j+l\leqslant 2}} k_{ijl}x^iy^jz^l,$$

and the following holds:

$$\frac{\partial F}{\partial x}y+\frac{\partial F}{\partial y}\big(x-x^3+by-kz\big)+\frac{\partial F}{\partial z}w(y-z)=KF. \tag{2}$$

By equating the coefficients of the monomials on both sides of (2), we obtain a system of 84 equations in 48 unknowns, namely the 35 coefficients a_{ijl}, the 10 cofactor coefficients k_{ijl}, and the parameters b, k, and w.

Solving this system with the help of a computer algebra system such as Mathematica or Maple, and taking into account Proposition 4, we obtain the six irreducible invariant algebraic surfaces $F_i=0$, with F_i shown in Table 1.

This concludes the proof of the proposition. □

We remark that the case with the invariant algebraic surface F_4 corresponds to the case with F_3 by applying the symmetry $(x,y,z,t,b,k,w)\to(-x,-y,-z,-t,-b,-k,-w)$. The same occurs in the cases with the invariant algebraic surfaces F_5 and F_6. Then the study of the systems with the invariant algebraic surfaces F_3 and F_5 is enough to determine also the behavior in the cases with F_4 and F_6.

A *first integral* of systems (1) is a (nonlocally constant) continuously differentiable function $H:A\to\mathbb{R}$, where A is an open and dense subset of $\mathbb{R}^3$, which remains constant along all solutions $(x(t),y(t),z(t))$ of systems (1) that are contained in A; that is, such that

$$\frac{\partial H}{\partial x}y+\frac{\partial H}{\partial y}\big(x-x^3+by-kz\big)+\frac{\partial H}{\partial z}w(y-z)=0.$$

A first integral is called *simple* if it is not a function of other first integrals, and the first integral H is called *polynomial* if H is a polynomial function. The *degree* of a polynomial first integral is the degree of the polynomial.

In what follows, we describe all polynomial first integrals of degree at most four of systems (1).

Proposition 2. *All simple polynomial first integrals of degree at most four of systems* (1) *are given in Table* 2.

Table 2. Simple polynomial first integrals of systems (1), $H_i=H_i(x,y,z)$ for $1\leqslant i\leqslant 2$.

Conditions	Simple polynomial first integral
$b=0, k=0$	$H_1=2x^2-x^4-2y^2$
$w=0$	$H_2=z$

Table 3. Darboux invariants of systems (1), $I_i = I_i(x, y, z)$ for $1 \leqslant i \leqslant 4$.

Conditions	Darboux invariant
$b = -w = -\frac{3}{\sqrt{22}}, k = -\frac{4}{\sqrt{22}}$	$I_1 = (\sqrt{22}x^2 - \sqrt{22}x^4 - 4xy - 2\sqrt{22}y^2 + 16xz)\mathrm{e}^{(4/\sqrt{22})t}$
$b = -w = \frac{3}{\sqrt{22}}, k = \frac{4}{\sqrt{22}}$	$I_2 = (\sqrt{22}x^2 - \sqrt{22}x^4 + 4xy - 2\sqrt{22}y^2 - 16xz)\mathrm{e}^{-(4/\sqrt{22})t}$
$b = -\sqrt{\frac{3}{2}}, k = -2\sqrt{\frac{2}{3}}, w = \sqrt{\frac{2}{3}}$	$I_3 = (\sqrt{6}x^2 - \sqrt{6}x^4 - 4xy - 2\sqrt{6}y^2 + 8xz + 2\sqrt{6}z^2)\mathrm{e}^{2\sqrt{2/3}t}$
$b = \sqrt{\frac{3}{2}}, k = 2\sqrt{\frac{2}{3}}, w = -\sqrt{\frac{2}{3}}$	$I_4 = (\sqrt{6}x^2 - \sqrt{6}x^4 + 4xy - 2\sqrt{6}y^2 - 8xz + 2\sqrt{6}z^2)\mathrm{e}^{-2\sqrt{2/3}t}$

Proof. Given that a polynomial first integral corresponds either to an invariant algebraic surface with zero cofactor, or to a combination of the invariant algebraic surfaces with respective nonzero cofactors whose sum is zero, the result stated in Proposition 2 follows directly from Proposition 1, Table 1, and Proposition 4. □

The differential systems (1) are said to be *completely integrable* if there exist two functionally independent first integrals; that is, their gradients are linearly independent except possibly on a set of Lebesgue measure zero.

Corollary 1. *The differential systems* (1) *are completely integrable if* $b = k = w = 0$*, with the two first integrals* H_1 *and* H_2 *of Table* 2*.*

Proof. According to Table 2, the systems described by (1) with parameters $b = k = w = 0$ possess two polynomial first integrals, H_1 and H_2. These integrals are evidently independent, as H_1 does not involve the variable z, whereas H_2 explicitly depends on them. This establishes the validity of Corollary 1. □

An *invariant* of systems (1) defined on an open and dense subset $A \subset \mathbb{R}^3$ is a nonconstant C^1 function, $I = I(x, y, z, t)$, such that $I(x(t), y(t), z(t), t)$ remains constant along any solutions $(x(t), y(t), z(t))$ of systems (1) contained in A, i.e.,

$$\frac{\partial I}{\partial x}y + \frac{\partial I}{\partial y}\big(x - x^3 + by - kz\big) + \frac{\partial I}{\partial z}w(y - z) + \frac{\partial I}{\partial t} = 0$$

for all $(x(t), y(t), z(t)) \in A$. Note that if an invariant is independent of t, it is a first integral.

An invariant of the form $I = f(x, y, z)\mathrm{e}^{st}$, where f is an analytic function in A and $s \in \mathbb{R} \setminus \{0\}$, is called a *Darboux invariant*. A Darboux invariant is said to be *simple* if it cannot be written as a function of other Darboux invariants.

Proposition 3. *All Darboux invariants of the form* $I = f(x, y, z)\mathrm{e}^{st}$*, where* $f(x, y, z)$ *is composed of the polynomials* F_i*, with* $i = 1, 2, 3, 4$*, listed in Table* 1 *are summarized in Table* 3*.*

Proof. The proof of this result follows directly from Proposition 5 and from the irreducible invariant surfaces obtained in Proposition 2, which have a nonzero constant cofactor. To apply Proposition 5, it has been taken into account that, when the values of the parameters b, k, and w defining the equation are fixed, there exists at most one irreducible invariant surface of degree less than or equal to 4. □

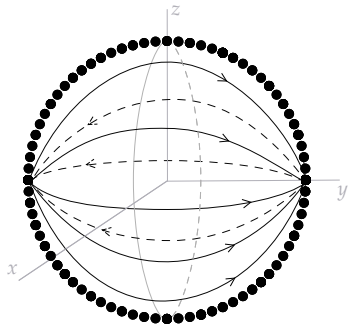

Figure 1. Dynamics of systems (1) on the infinite sphere.

Let $\varphi_p(t)$ be the solution of systems (1) such that $\varphi_p(0) = p$, defined on its maximal interval (α_p, ω_p). If $\omega_p = +\infty$, we define the ω-limit set of p as

$$\omega(p) = \Big\{q \in \mathbb{R}^3\colon\ \exists\{t_n\} \subset \mathbb{R} \text{ with } \lim_{n\to\infty} t_n = +\infty \text{ and } \lim_{n\to\infty} \varphi_p(t_n) = q\Big\}.$$

In the same way, if $\alpha_p = -\infty$, we define the α-limit set of p as

$$\alpha(p) = \Big\{q \in \mathbb{R}^3\colon\ \exists\{t_n\} \subset \mathbb{R} \text{ with } \lim_{n\to\infty} t_n = -\infty \text{ and } \lim_{n\to\infty} \varphi_p(t_n) = q\Big\}.$$

The presence of a first integral enables a reduction of the phase space dimension by one when analyzing the dynamics of a differential system. In contrast, a Darboux invariant provides valuable information about the α- and ω-limits behavior of the system's trajectories; see [5, Prop. 5] or Proposition 6 in Section 2.

We recall that an equilibrium point of a planar system is called a *center* if there is an open neighborhood, called the *period annulus*, consisting, besides the equilibrium point, of periodic orbits. If this neighborhood is all the plane $\mathbb{R}^2$, then we say that the equilibrium is a *global center*.

Theorem 1. *The phase portrait of the family of systems* (1) *on the infinite sphere is as shown in Fig.* 1. *The infinity of the plane $x = 0$ is filled with equilibria. The orbits in the region $x < 0$ have their α-limit in the endpoint of the positive y-axis and their ω-limit in the endpoint of the negative y-axis. The orbits in the region $x > 0$ have their α-limit in the endpoint of the negative y-axis and their ω-limit in the endpoint of the positive y-axis.*

Theorem 1 is proved in Section 3.

The following result shows the global dynamics of systems (1) in the case $w = 0$, in which there exists a first integral $H_2 = z$ that allows the reduction of systems (1) to a family of planar polynomial systems.

Theorem 2. *The differential system*

$$\dot{x} = y, \qquad \dot{y} = x - x^3 + by - \big(s - s^3\big), \tag{3}$$

with $s \in \mathbb{R}$, has at infinity a unique pair of equilibria at the origins of the local charts U_2 and V_2. Their local phase portraits are formed by two hyperbolic sectors with both

separatrices at infinity. The following statements hold for the differential system (3):

(a) *When* $|s| > 2/\sqrt{3}$, *the system has the unique finite equilibrium* $P_1 = (s, 0)$. *Then, if* $b \in (-2\sqrt{3s^2-1}, 2\sqrt{3s^2-1})$, *the phase portrait in the Poincaré disc is a global hyperbolic unstable focus if* $b > 0$, *a global Hamiltonian center if* $b = 0$, *and a global hyperbolic stable focus if* $b < 0$. *If* $b \in \mathbb{R}\backslash(-2\sqrt{3s^2-1}, 2\sqrt{3s^2-1})$, *the phase portrait in the Poincaré disc is a global hyperbolic unstable node if* $b > 0$ *and a global hyperbolic stable node if* $b < 0$.

(b) *If* $|s| = 2/\sqrt{3}$, *in addition to the finite equilibrium point* P_1, *the system has another equilibrium point* $P_2 = (-s/2, 0)$. *If* $b \in (-2\sqrt{3}, 2\sqrt{3})$, *then if* $b > 0$, P_1 *is a hyperbolic unstable focus and* P_2 *is a semihyperbolic saddle-node. If* $b = 0$, *then* P_1 *is a Hamiltonian center and* P_2 *is a nilpotent cusp, its two separatrices connect forming a homoclinic orbit, the boundary of the period annulus of the center. If* $b < 0$, *then* P_1 *is a hyperbolic stable focus and* P_2 *is a semihyperbolic saddle-node. If* $b \in \mathbb{R} \setminus (-2\sqrt{3}, 2\sqrt{3})$, *then if* $b > 0$, P_1 *is a hyperbolic unstable node and* P_2 *is a semihyperbolic saddle-node, and if* $b < 0$, *then* P_1 *is a hyperbolic stable node and* P_2 *is a semihyperbolic saddle-node.*

(c) *If* $|s| < 2/\sqrt{3}$, *in addition to the finite equilibrium point* P_1, *there are two finite equilibria* $P_3 = (-s - \sqrt{4-3s^2}/2, 0)$ *and* $P_4 = (-s + \sqrt{4-3s^2}/2, 0)$.

(c.1) *Assume that* $s \in (-2/\sqrt{3}, -1/\sqrt{3})$ *and* $b \in (-2\sqrt{3s^2-1}, 2\sqrt{3s^2-1})$. *Then, if* $b > 0$, P_1 *is a hyperbolic unstable focus,* P_3 *is a hyperbolic saddle and* P_4 *is a hyperbolic unstable focus if* $\alpha^+ = b^2 - 8 + 6s(s + \sqrt{4-3s^2}) < 0$, *and a hyperbolic unstable node if* $\alpha^+ \geqslant 0$. *If* $b = 0$, *then* P_1 *and* P_4 *are Hamiltonian centers and* P_3 *is a hyperbolic saddle. If* $b < 0$, *then* P_1 *is a hyperbolic stable focus,* P_3 *is a hyperbolic saddle and* P_4 *is a hyperbolic stable focus if* $\alpha^+ < 0$, *and a hyperbolic stable node if* $\alpha^+ \geqslant 0$.

(c.2) *Assume that* $s \in (-2/\sqrt{3}, -1/\sqrt{3})$ *and* $b \in \mathbb{R}\backslash(-2\sqrt{3s^2-1}, 2\sqrt{3s^2-1})$. *Then, if* $b > 0$, P_1 *is a hyperbolic unstable node,* P_3 *is a hyperbolic saddle and* P_4 *is a hyperbolic unstable focus if* $\alpha^+ < 0$, *and a hyperbolic unstable node if* $\alpha^+ \geqslant 0$. *If* $b < 0$, *then* P_1 *is a hyperbolic stable node,* P_3 *is a hyperbolic saddle and* P_4 *is a hyperbolic stable focus if* $\alpha^+ < 0$, *and a hyperbolic stable node if* $\alpha^+ \geqslant 0$.

(c.3) *Assume that* $s = -1/\sqrt{3}$. *If* $b > 0$, *then the equilibrium* $P_1 = P_3$ *is a semihyperbolic saddle-node and* P_4 *is a hyperbolic unstable node. If* $b = 0$, *then the equilibrium* $P_1 = P_3$ *is a cusp and* P_4 *is a Hamiltonian center. If* $b < 0$, *then the equilibrium* $P_1 = P_3$ *is a semihyperbolic saddle-node and* P_4 *is a hyperbolic stable node.*

(c.4) *Assume that* $s \in (-1/\sqrt{3}, 1/\sqrt{3})$. *In this case,* P_1 *is a hyperbolic saddle. If* $b = 0$, *then* P_3 *and* P_4 *are Hamiltonian centers. If* $\alpha^- = b^2 - 8 + 6s(s - \sqrt{4-3s^2}) < 0$ *and* $\alpha^+ < 0$, *then if* $b > 0$, P_3 *and* P_4 *are hyperbolic unstable foci, and if* $b < 0$, P_3 *and* P_4 *are hyperbolic stable foci. If* $\alpha^- < 0$ *and* $\alpha^+ \geqslant 0$, *then if* $b > 0$, P_3 *is a hyperbolic unstable focus and* P_4 *a hyperbolic unstable node; if* $b < 0$, P_3 *is a hyperbolic stable focus and* P_4 *a hyperbolic stable node. If* $\alpha^- \geqslant 0$ *and* $\alpha^+ < 0$, *then if* $b > 0$, P_3 *is*

a hyperbolic unstable node and P_4 a hyperbolic unstable focus; if $b < 0$, P_3 is a hyperbolic stable node and P_4 a hyperbolic stable focus. If $\alpha^- \geqslant 0$ and $\alpha^+ \geqslant 0$, then if $b > 0$, P_3 and P_4 are hyperbolic unstable nodes, and if $b < 0$, P_3 and P_4 are hyperbolic stable nodes.

(c.5) *Assume that $s = 1/\sqrt{3}$. If $b > 0$, then the equilibrium $P_1 = P_4$ is a semihyperbolic saddle-node and P_3 is a hyperbolic unstable node. If $b = 0$, then the equilibrium $P_1 = P_4$ is a cusp, and P_3 is a Hamiltonian center. If $b < 0$, the equilibrium $P_1 = P_4$ is semihyperbolic saddle-node and P_3 is a hyperbolic stable node.*

(c.6) *Assume that $s \in (1/\sqrt{3}, 2/\sqrt{3})$ and $b \in (-2\sqrt{3s^2-1}, 2\sqrt{3s^2-1})$. Then, if $b > 0$, P_1 is a hyperbolic unstable focus, P_4 is a hyperbolic saddle and P_3 is a hyperbolic unstable focus if $\alpha^- < 0$, and a hyperbolic unstable node if $\alpha^- \geqslant 0$. If $b = 0$, then P_1 and P_3 are Hamiltonian centers and P_4 is a hyperbolic saddle. If $b < 0$, then P_1 is a hyperbolic stable focus, P_4 is a hyperbolic saddle and P_3 is a hyperbolic stable focus if $\alpha^- < 0$, and a hyperbolic stable node if $\alpha^- \geqslant 0$.*

(c.7) *Assume that $s \in (1/\sqrt{3}, 2/\sqrt{3})$ and $b \in \mathbb{R} \setminus (-2\sqrt{3s^2-1}, 2\sqrt{3s^2-1})$. Then, if $b > 0$, P_1 is a hyperbolic unstable node, P_4 is a hyperbolic saddle and P_3 is a hyperbolic unstable focus if $\alpha^- < 0$, and a hyperbolic unstable node if $\alpha^- \geqslant 0$. If $b < 0$, then P_1 is a hyperbolic stable node, P_4 is a hyperbolic saddle and P_3 is a hyperbolic stable focus if $\alpha^- < 0$, and a hyperbolic stable node if $\alpha^- \geqslant 0$.*

There are six topologically different phase portraits of system (3) *in the Poincaré disc, which are included in Figs.* 2–3. *For $s \in (-2/\sqrt{3}, 2/\sqrt{3})$, if $b \neq 0$, the phase portrait in the Poincaré disc is topologically equivalent to G1, and if $b = 0$, it is topologically equivalent to G2. For $|s| = 2/\sqrt{3}$, if $b \neq 0$, the phase portrait in the Poincaré disc is topologically equivalent to G3, and if $b = 0$, it is topologically equivalent to G4. Finally, for $s \in \mathbb{R} \setminus (-2/\sqrt{3}, 2/\sqrt{3})$, if $b \neq 0$, the phase portrait in the Poincaré disc is topologically equivalent to G5, and if $b = 0$, it is topologically equivalent to G6.*

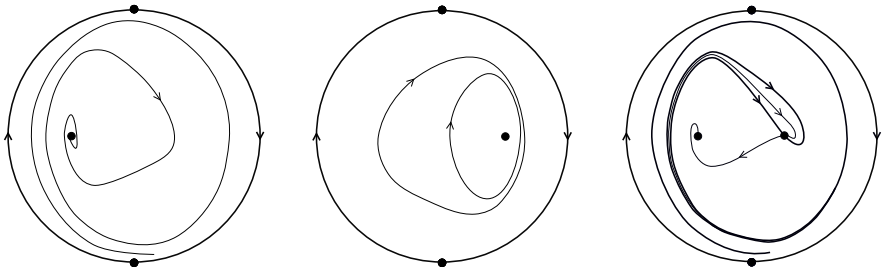

G1 $s \in (-2/\sqrt{3}, 2/\sqrt{3}), b \neq 0$ | G2 $s \in (-2/\sqrt{3}, 2/\sqrt{3}), b = 0$ | G3 $s = \|2/\sqrt{3}\|, b \neq 0$

Figure 2. Phase portraits of system (3) in the Poincaré disc: G1–G3.

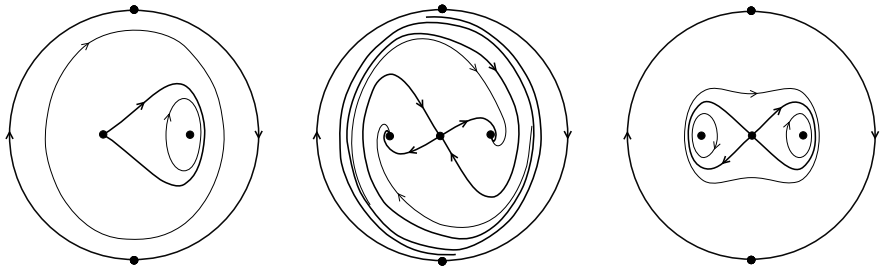

G4 $s = |2/\sqrt{3}|, b = 0$ | G5 $s \in \mathbb{R} \setminus (-2\sqrt{3}, 2\sqrt{3}), b \neq 0$ | G6 $s \in \mathbb{R} \setminus (-2/\sqrt{3}, 2/\sqrt{3}), b = 0$

Figure 3. Phase portraits of system (3) in the Poincaré disc: G4–G6.

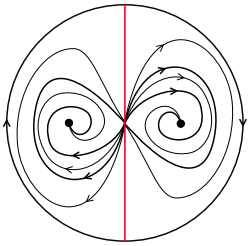

Figure 4. Global phase portrait of systems (1) on the invariant surface $F_3 = 0$ when $b = -w = -3/\sqrt{22}$ and $k = -4/\sqrt{22}$.

Theorem 2 is proved in Section 4.

Systems (1) under the conditions $b = -w = -3/\sqrt{22}$ and $k = -4/\sqrt{22}$ have the Darboux invariant

$$I_1 = \left(\sqrt{22}x^2 - \sqrt{22}x^4 - 4xy - 2\sqrt{22}y^2 + 16xz\right)\mathrm{e}^{4/\sqrt{22}t}.$$

In the next theorem, we characterize its dynamics in the Poincaré ball.

Theorem 3. *The global dynamics of system* (1) *under the conditions*

$$b = -w = -\frac{3}{\sqrt{22}} \quad \textit{and} \quad k = -\frac{4}{\sqrt{22}}$$

is described below:

(a) *The phase portrait on the Poincaré disc at the invariant algebraic surface* $F_3(x, y) = \sqrt{22}x^2 - \sqrt{22}x^4 - 4xy - 2\sqrt{22}y^2 + 16xz = 0$ *is the one given in Fig.* 4.

(b) *The* ω*-limit of a point* $p = (x_0, y_0, z_0)$*, which is not on the surface* $F_3 = 0$*, is the point* $(-1, 0, 0)$ *if* $x_0, y_0 < 0$*; the point* $(1, 0, 0)$ *if* $x_0, y_0 > 0$*; and either* $(-1, 0, 0)$*,* $(1, 0, 0)$*,* $(0, 0, 0)$ *or the endpoints of the* y*-axis, if* $x_0 y_0 < 0$*. The* α*-limit of any point* p *is one of the endpoints of the* y*-axis.*

Note that the dynamics on the infinite sphere is shown in Theorem 1.

Theorem 3 is proved in Section 5.

2 Preliminaries

2.1 Poincaré compactification

2.1.1 Poincaré compactification in dimension 2

In this subsection, we present the Poincaré compactification, a technique that enables the study of the behavior of the trajectories of a polynomial differential system near infinity. This method will be applied in Sections 4 and 5.

We begin by considering the unit sphere $\mathbb{S}^2 = \{y \in \mathbb{R}^3 \colon y_1^2 + y_2^2 + y_3^2 = 1\}$, hereafter called the *Poincaré sphere*. The tangent plane to the sphere at the point $(0, 0, 1)$ is identified with the Euclidean plane $\mathbb{R}^2$, where we consider the polynomial system of degree d

$$\dot{x}_1 = P_1(x_1, x_2), \qquad \dot{x}_2 = P_2(x_1, x_2).$$

This planar system induces a vector field on the northern and southern hemispheres of the sphere via the central projections $f^+ \colon \mathbb{R}^2 \to \mathbb{S}^2$ and $f^- \colon \mathbb{R}^2 \to \mathbb{S}^2$, defined by $f^{\pm}(x) = \pm(x_1, x_2, 1)/\Delta(x)$ with $\Delta(x) = \sqrt{x_1^2 + x_2^2 + 1}$. Through the differentials of these maps, we obtain the corresponding vector fields on these hemispheres.

By multiplying the vector field by y_3^d, it is possible to extend it analytically to the equator of the sphere, which corresponds to the points at infinity of the original plane $\mathbb{R}^2$.

This analytic extension is known as the *Poincaré compactification* of the initial vector field. Analyzing the behavior of this extended field near the equator (i.e., near the circle $\mathbb{S}^1 = \{\mathbb{S}^2 \cap \{y_3 = 0\}\}$) allows to describe the dynamics of the original system close to infinity.

To perform computations, we work in the local charts (U_i, ϕ_i) and (V_i, ψ_i) of the sphere $\mathbb{S}^2$, defined as follows: $U_i = \{y \in \mathbb{S}^2 \colon y_i > 0\}$, $V_i = \{y \in \mathbb{S}^2 \colon y_i < 0\}$, with the maps $\phi_i : U_i \to \mathbb{R}^2$ and $\psi_i : V_i \to \mathbb{R}^2$ given by $\phi_i(y) = \psi_i(y) = (y_m/y_i, y_n/y_i)$, where $m < n$ are such that $m, n \neq i$ for $i = 1, 2$.

The expression of the Poincaré compactification in the local chart (U_1, ϕ_1) is

$$(\dot{u}, \dot{v}) = v^d(-uP_1 + P_2, -vP_1), \quad P_i = P_i\left(\frac{1}{v}, \frac{u}{v}\right),$$

and in the local chart (U_2, ϕ_2) is

$$(\dot{u}, \dot{v}) = v^d(-uP_2 + P_1, -vP_2), \quad P_i = P_i\left(\frac{u}{v}, \frac{1}{v}\right).$$

Considering the definitions of the local charts V_i and the maps ψ_i, one finds that the expression for the Poincaré compactification in the local charts (V_i, ψ_i), with $i = 1, 2$, is the same as in the local charts (U_i, ϕ_i) multiplied by $(-1)^{d-1}$.

Since our goal is to analyze the dynamics of the system near infinity, we focus on the so-called *infinite equilibrium points*, that is, the equilibrium points of the Poincaré compactification located on the equator $\mathbb{S}^1$ of the sphere. If a point $y \in \mathbb{S}^1$ is such an equilibrium, then its antipodal point $-y$ is also an equilibrium. The stability of this pair,

whether identical or opposite, depends on the degree of the original polynomial system. Therefore, to carry out a complete analysis, it suffices to examine the infinite equilibria in the local chart U_1 and the origin in the local chart U_2.

For a more detailed exposition of the Poincaré compactification in two dimensions, see [3, Chap. 5].

2.1.2 Poincaré compactification in dimension 3

The technique of the Poincaré compactification can be extended to higher dimensions. In particular, we use this technique in dimension 3 in Section 3. As the ideas are the same explained before, we just include here the expressions obtained in the local charts U_1, U_2, and U_3 for a polynomial system in $\mathbb{R}^3$ of degree d

$$\dot{x} = P_1(x, y, z), \qquad \dot{y} = P_2(x, y, z), \qquad \dot{z} = P_3(x, y, z).$$

More details about the Poincaré compactification in dimension n can be found in [1].

The phase portrait in the local chart U_1 is given by the system

$$(\dot{u}, \dot{v}, \dot{w}) = w^d(-uP_1 + P_2, -vP_1 + P_3, -wP_1), \quad P_i = P_i\left(\frac{1}{w}, \frac{u}{w}, \frac{v}{w}\right).$$

The phase portrait in the local chart U_2 is given by the system

$$(\dot{u}, \dot{v}, \dot{w}) = w^d(-uP_2 + P_1, -vP_2 + P_3, -wP_2), \quad P_i = P_i\left(\frac{u}{w}, \frac{1}{w}, \frac{v}{w}\right).$$

In the local chart U_3, the phase portrait is given by

$$(\dot{u}, \dot{v}, \dot{w}) = w^d(-uP_3 + P_1, -vP_3 + P_2, -wP_3), \quad P_i = P_i\left(\frac{u}{w}, \frac{v}{w}, \frac{1}{w}\right).$$

The following result is proved in [4].

Lemma 1. *Let $f(x, y, z) = 0$ be an algebraic surface of degree m in $\mathbb{R}^3$. The extension of this surface to the boundary of the Poincaré ball is contained in the surface defined by*

$$w^m f\left(\frac{x}{w}, \frac{y}{w}, \frac{z}{w}\right) = 0, \qquad w = 0.$$

2.2 Invariant algebraic surfaces and Darboux invariants

We will use the following results (see Theorem 8.4 and Proposition 8.7 of [3], respectively, for a proof).

Proposition 4. *Suppose $f \in \mathbb{R}[x, y, z]$, and let $f = f_1^{n_1} \cdots f_r^{n_r}$ be its factorization into irreducible factors over $\mathbb{R}[x, y, z]$. Then, for the family of polynomial differential systems* (1)*, $f = 0$ is an invariant algebraic surface with cofactor K_f if and only if $f_i = 0$ is an invariant algebraic surface for each $i = 1, \ldots, r$ with cofactor K_{f_i}. Moreover, $K_f = n_1 K_{f_1} + \cdots + n_r K_{f_r}$.*

Proposition 5. *Assume that systems* (1) *admit* p *irreducible invariant algebraic surfaces* $f_i = 0$ *with cofactors* K_i *for* $i = 1, \dots, p$*, not all zero, such that* $\sum_{i=1}^{p} \lambda_i K_i = -s$ *for some* $s \in \mathbb{R} \setminus \{0\}$*. Then the function*

$$f_1^{\lambda_1} \cdots f_p^{\lambda_p} \mathrm{e}^{st}$$

is a Darboux invariant of systems (1)*.*

The following proposition is the Proposition 5 of [5].

Proposition 6. *Let* $\mathbb{S}^2$ *be the infinity of the Poincaré ball and* $I(x, y, z, t) = f(x, y, z)\mathrm{e}^{st}$ *be a Darboux invariant of systems* (1)*. Let also* $p \in \mathbb{R}^3$*, and let* $\phi_p(t)$ *be the solution of systems* (1) *such that* $\phi_p(0) = p$*, with maximal interval* $(-\infty, \infty)$*, because the Poincaré ball is compact. Then the following holds*:

(i) *Assume that* $s > 0$*. Then* $\omega(p)$ *is contained in the closure* $\overline{\{f(x, y, z) = 0\}}$ *in the Poincaré ball, and* $\alpha(p) \subset \overline{\{f(x, y, z) = 0\}} \cap \mathbb{S}^2$*, being* $\mathbb{S}^2$ *the boundary of the Poincaré ball.*

(ii) *Assume that* $s < 0$*. Then* $\alpha(p)$ *is contained in* $\overline{\{f(x, y, z) = 0\}}$*, and* $\omega(p) \subset \overline{\{f(x, y, z) = 0\}} \cap \mathbb{S}^2$.

3 Proof of Theorem 1

The expression of the Poincaré compactification of systems (1) in the local chart U_1 is

$$\begin{aligned}
\dot{z}_1 &= -1 + z_3^2 + bz_1 z_3^2 - kz_2 z_3^2 - z_1^2 z_3^2,\\
\dot{z}_2 &= wz_1 z_3^2 - wz_2 z_3^2 - z_1 z_2 z_3^2,\\
\dot{z}_3 &= z_1 z_3^2.
\end{aligned}$$

Then, as $\dot{z}_1 \mid_{z_3=0} = -1$, there are not infinite equilibria on the local chart U_1.

The expression of the Poincaré compactification of systems (1) in the local chart U_2 is

$$\begin{aligned}
\dot{z}_1 &= z_3^2 - bz_1 z_3^2 + z_1^4 - z_1^2 z_3^2 + kz_1 z_2 z_3^2,\\
\dot{z}_2 &= wz_3^2 - (b + w)z_2 z_3^2 + z_1^3 z_2 - z_1 z_2 z_3^2 + kz_2^2 z_3^2,\\
\dot{z}_3 &= bz_3^3 - z_1^3 z_3 + z_1 z_3^3 - kz_2 z_3^3.
\end{aligned}$$

At infinity, i.e., when $z_3 = 0$, this system is written as

$$\dot{z}_1 = z_1^4, \qquad \dot{z}_2 = z_1^3 z_2. \tag{4}$$

The line $z_1 = 0$ if filled with equilibria. With a change of the time variable, we remove the common factor z_1^3, and we get the system

$$\dot{z}_1 = z_1, \qquad \dot{z}_2 = z_2. \tag{5}$$

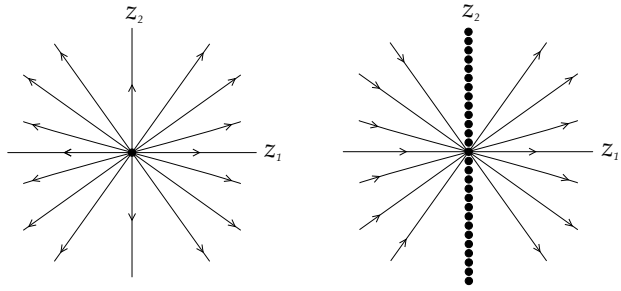

(a) (b)

Figure 5. Phase portraits of system (5) in (a) and system (4) in (b).

The only remaining equilibrium point in system (5) is the origin, which is a hyperbolic unstable star node, as in Fig. 5(a). Multiplying by z_3, we obtain the phase portrait around the line $z_1 = 0$ for system (4), given in Fig. 5(b).

The expression of the Poincaré compactification of systems (1) in the local chart U_3 is

$$\begin{aligned}
\dot{z}_1 &= wz_1z_3^2 + z_2z_3^2 - wz_1z_2z_3^2,\\
\dot{z}_2 &= -kz_3^2 - z_1^3 + z_1z_3^2 + (b+w)z_2z_3^2 - wz_2^2z_3^2,\\
\dot{z}_3 &= -wz_3^3 + wz_2z_3^3.
\end{aligned}$$

At infinity, i.e., when $z_3 = 0$ this system becomes

$$\dot{z}_1 = 0, \qquad \dot{z}_2 = -z_1^3.$$

Again, the line $z_1 = 0$ is filled with equilibria, and the orbits are along the straight lines with constant z_1.

Combining the information in the three local charts (and the corresponding V_1, V_2, and V_3), on the infinite sphere, the plane $x = 0$ is filled with equilibria, and all the other orbits have their α- and ω-limits at the origins of charts U_2 or V_2. More precisely: the orbits in the region $x > 0$ have their α-limit in the origin of the local chart V_2, i.e., in the endpoint of the negative y-axis, and their ω-limit in the origin of the local chart U_2, i.e., in the endpoint of the positive y-axis. The orbits in the region $x < 0$ have their α-limit in the endpoint of the positive y-axis and their ω-limit in the endpoint of the negative y-axis.

4 Proof of Theorem 2

The family of systems (1) with $w = 0$ has the first integral $H_2 = z$, so on any level $H_2 = z = h$, we can reduce systems (1) to the planar polynomial family of systems (3), where we have rewritten the constant term kh in $\dot{y}$ as $s - s^3$ in order to simplify the computations. In this section, we study the dynamics of systems (3) in the Poincaré disc for any value of $s, b \in \mathbb{R}$.

Finite equilibrium points

If $s \in (-\infty, -2/\sqrt{3}) \cup (2/\sqrt{3}, \infty)$, systems (3) have the unique finite equilibrium point $P_1 = (s, 0)$. If $s = \pm 2/\sqrt{3}$, systems (3) have, in addition to P_1, the equilibrium point $P_2 = (-s/2, 0)$. If $s \in (-2/\sqrt{3}, 2/\sqrt{3})$, systems (3) have three finite equilibrium points: P_1, $P_3 = ((-s - \sqrt{4 - 3s^2})/2, 0)$, and $P_4 = ((-s + \sqrt{4 - 3s^2})/2, 0)$.

For the equilibrium point P_1, if $s \in (-1/\sqrt{3}, 1/\sqrt{3})$, it is a hyperbolic saddle. If $s \in \mathbb{R} \setminus (-1/\sqrt{3}, 1/\sqrt{3})$, we will distinguish two cases. If $b \in (-2\sqrt{3s^2 - 1}, 2\sqrt{3s^2 - 1})$, then P_1 is a hyperbolic stable focus if $b < 0$, a hyperbolic unstable focus if $b > 0$, and a Hamiltonian center if $b = 0$. On the other hand, if $b \in \mathbb{R} \setminus (-2\sqrt{3s^2 - 1}, 2\sqrt{3s^2 - 1})$, then P_1 is a hyperbolic stable node if $b < 0$, and a hyperbolic unstable node if $b > 0$. This leads to statement (a) of Theorem 2. If $s = \pm 1/\sqrt{3}$ and $b \neq 0$, then P_1 is semihyperbolic, and applying [3, Thm. 2.19], we conclude that it is a saddle-node; finally, if $s = \pm 1/\sqrt{3}$ and $b = 0$, P_1 is nilpotent, and applying [3, Thm. 3.5], it is a cusp.

The equilibrium point P_2 is semihyperbolic if $b \neq 0$ and nilpotent if $b = 0$. Applying the mentioned results in [3], we determine that P_2 is a saddle-node if $b \neq 0$, and a cusp if $b = 0$. This leads to statement (b) in Theorem 2.

The equilibrium point P_3 is a hyperbolic saddle if $s \in (-2/\sqrt{3}, -1/\sqrt{3})$. If $s = -1/\sqrt{3}$, then $P_3 = P_1$. If $s \in (-1/\sqrt{3}, 2/\sqrt{3})$ and $\alpha^- = b^2 - 8 + 6s(s - \sqrt{4 - 3s^2}) < 0$, then P_3 is a hyperbolic stable focus if $b < 0$, a hyperbolic unstable focus if $b > 0$, and a Hamiltonian center if $b = 0$. If $\alpha^- \geqslant 0$, then P_3 is a hyperbolic stable node if $b < 0$, and a hyperbolic unstable node if $b > 0$.

For the equilibrium point P_4, if $s \in (-2/\sqrt{3}, 1/\sqrt{3})$ and $\alpha^+ = b^2 - 8 + 6s(s + \sqrt{4 - 3s^2}) < 0$, then P_4 is a hyperbolic stable focus if $b < 0$, a hyperbolic unstable focus if $b > 0$, and a Hamiltonian center if $b = 0$. If $\alpha^+ \geqslant 0$, then P_4 is a hyperbolic stable node if $b < 0$, and a hyperbolic unstable node if $b > 0$. If $s = 1/\sqrt{3}$, then $P_4 = P_1$. Finally, if $s \in (1/\sqrt{3}, 2/\sqrt{3})$, P_4 is a hyperbolic saddle.

Combining these conclusions about P_3 and P_4 with those for P_1, we get statement (c) in Theorem 2.

Infinite equilibrium points

Here we want to study the dynamics of systems (3) at infinity, and we will consider the Poincaré compactification introduced in Subsection 2.1.1.

In the local chart U_1, systems (3) have the expression

$$\dot{u} = -1 + v^2 + buv^2 - \left(s - s^3\right)v^3 - u^2v^2, \qquad \dot{v} = -uv^3,$$

so there are not infinite equilibrium points in the local chart U_1.

In the local chart U_2, systems (3) have the expression

$$\begin{aligned} \dot{u} &= v^2 - buv^2 + u^4 - u^2v^2 + \left(s - s^3\right)uv^3, \\ \dot{v} &= -bv^3 + u^3v - uv^3 + \left(s - s^3\right)v^4. \end{aligned} \tag{6}$$

The only point we need to study in the local chart U_2 is the origin, and it is linearly zero.

We will study the local phase portrait at the origin of the chart U_2 doing vertical blow-ups. Since $u=0$ is a characteristic direction, we need to do a twist $(u,v)=(u_1-v_1,v_1)$. In the new coordinates (u_1,v_1), system (6) becomes

$$\begin{aligned}\dot{u}_1 &= v_1^2 - bu_1v_1^2 + u_1^4 - 3u_1^3v_1 + 2u_1^2v_1^2 + cu_1v_1^3,\\ \dot{v}_1 &= -bv_1^3 + u_1^3v_1 - 3u_1v_1^2 + 2u_1v_1^3 + cv_1^4.\end{aligned} \tag{7}$$

Now we perform the vertical blow-up $(u_1,v_1)=(u_2,u_2v_2)$, and system (7) becomes

$$\dot{u}_2 = u_2^4 + u_2^2v_2^2 - 3u_2^4v_2 - bu_2^3v_2^2 + 2u_2^4v_2^2 + cu_2^4v_2^3, \qquad \dot{v}_2 = -u_2v_2^3. \tag{8}$$

Since u_2 is a common factor of $\dot{u}_2$ and $\dot{v}_2$, we rescale the time, and we get the differential system

$$\dot{u}_2 = u_2^3 + u_2v_2^2 - 3u_2^3v_2 - bu_2^2v_2^2 + 2u_2^3v_2^2 + cu_2^3v_2^3, \qquad \dot{v}_2 = -v_2^3. \tag{9}$$

The only equilibrium point on the straight line $u_2=0$ is the origin, and it is linearly zero. We perform another vertical blow-up, but first we make a twist since $u_2=0$ is a characteristic direction. Then, taking $(u_2,v_2)=(u_3-v_3,v_3)$, system (9) becomes

$$\begin{aligned}\dot{u}_3 &= u_3^3 - 3u_3^2v_3 + 4u_3v_3^2 - 3v_3^3 - 3u_3^3v_3 + (9-b)u_3^2v_3^2 + (2b-9)u_3v_3^3\\ &\quad + (3-b)v_3^4 + 6u_3^2v_3^3 + 6u_3v_3^4 - 2v_3^5 + \big(s-s^3\big)u_3^3v_3^3 - 3\big(s-s^3\big)u_3^2v_3^4\\ &\quad + 3\big(s-s^3\big)u_3v_3^5 - \big(s-s^3\big)v_3^6,\\ \dot{v}_3 &= -v_3^3.\end{aligned} \tag{10}$$

Now we perform the vertical blow-up $(u_3,v_3)=(u_4,u_4v_4)$, and system (10) becomes

$$\begin{aligned}\dot{u} &= u_4^3 - 3u_4^4v_4 + 4u_4^3v_4^2 + (9-b)u_4^4v_4^2 - 3u_4^3v_4^3 + 2u_4^5v_4^2 + (2b-9)u_4^4v_4^3\\ &\quad - 3u_4^3v_4 - 6u_4^5v_4^3 + (3-b)u_4^4v_4^4 + \big(s-s^3\big)u_4^6v_4^3 + 6u_4^5v_4^4 - 3\big(s-s^3\big)u_4^6v_4^4\\ &\quad - 2u_4^5v_4^5 + 3\big(s-s^3\big)u_4^6v_4^5 - \big(s-s^3\big)u_4^6v_4^6,\\ \dot{v} &= -u_4^2v_4 + 3u_4^2v_4^2 + 3u_4^3v_4^2 - 5u_4^2v_4^3 + (b-9)u_4^3v_4^3 + 3u_4^2v_4^4 - 2u_4^4v_4^3\\ &\quad + (9-2b)u_4^3v_4^4 + 6u_4^4v_4^4 + (b-3)u_4^3v_4^5 - \big(s-s^3\big)u_4^5v_4^4 - 6u_4^4v_4^5\\ &\quad + 3\big(s-s^3\big)u_4^5v_4^5 + 2u_4^4v_4^6 - 3\big(s-s^3\big)u_4^5v_4^6 + \big(s-s^3\big)u_4^5v_4^7.\end{aligned} \tag{11}$$

Since u_4 is a common factor of $\dot{u}_4$ and $\dot{v}_4$, we rescale the time, and we get the differential system

$$\begin{aligned}\dot{u} &= u_4 - 3u_4^2v_4 + 4u_4v_4^2 + (9-b)u_4^2v_4^2 - 3u_4v_4^3 + 2u_4^3v_4^2 + (2b-9)u_4^2v_4^3\\ &\quad - 3u_4v_4 - 6u_4^3v_4^3 + (3-b)u_4^2v_4^4 + \big(s-s^3\big)u_4^4v_4^3 + 6u_4^3v_4^4 - 3\big(s-s^3\big)u_4^4v_4^4\\ &\quad - 2u_4^3v_4^5 + 3\big(s-s^3\big)u_4^4v_4^5 - \big(s-s^3\big)u_4^4v_4^6,\\ \dot{v} &= -v_4 + 3v_4^2 + 3u_4v_4^2 - 5v_4^3 + (b-9)u_4v_4^3 + 3v_4^4 - 2u_4^2v_4^3 + (9-2b)u_4v_4^4\\ &\quad + 6u_4^2v_4^4 + (b-3)u_4v_4^5 - (s-s^3)u_4^3v_4^4 - 6u_4^2v_4^5 + 3(s-s^3)u_4^3v_4^5 + 2u_4^2v_4^6\\ &\quad - 3(s-s^3)u_4^3v_4^6 + (s-s^3)u_4^3v_4^7.\end{aligned} \tag{12}$$

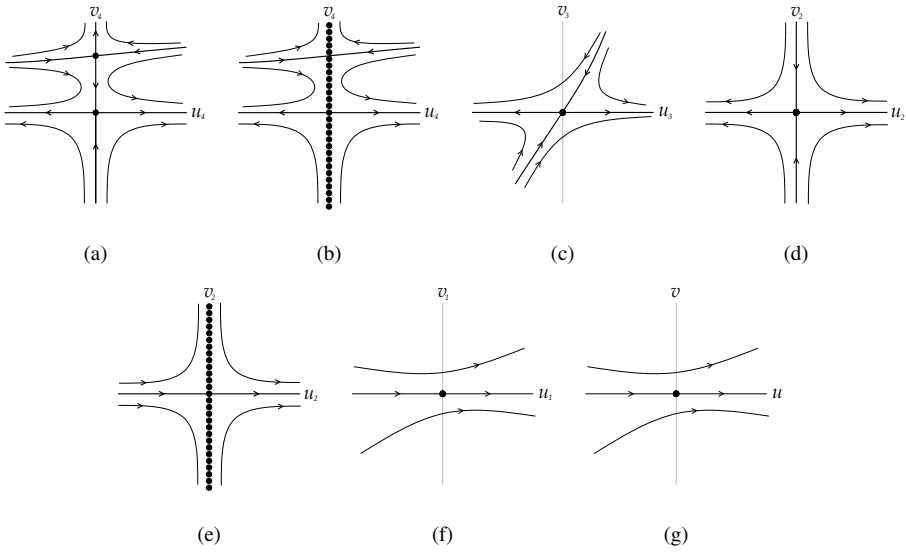

Figure 6. Blowing down of the origin of system (6).

There are two equilibrium points on $u_2 = 0$, the origin and the point $(0, 1)$, and both are hyperbolic saddles. Now we undo the blow-ups and twists.

For system (12), the local phase portrait in a neighborhood of the straight line $u_4 = 0$ is given in Fig. 6(a). If we multiply by u_4^2 to return to system (11), then all points on the u_4-axis become equilibrium points. Thus we obtain the phase portrait in Fig. 6(b) for system (11) around the straight line $u_4 = 0$. Now we undo the blow-up to obtain the local phase portrait at the origin of system (10), and we obtain the local phase portrait in Fig. 6(c) for system (10). If we undo the twist and return to system (9), we obtain the phase portrait in Fig. 6(d). If we multiply by u_2 to return to system (8), then all points on the u_2-axis become equilibrium points, and the orientation of the orbits in the second and third quadrants is reversed. Then we obtain the phase portrait in Fig. 6(e). Now we undo the blow-up to obtain the local phase portrait at the origin of system (7), and we obtain the local phase portrait in Fig. 6(f). Finally, if we undo the twist, we obtain the local phase portrait at the origin of the local chart U_2, which is given in Fig. 6(g).

Phase portraits in the Poincaré disc

Now we will prove the topological classification of all phase portraits of systems (3) stated in Theorem 2.

First, we note that systems (3) do not have limit cycles. The divergence of the systems is b, and then, if $b \neq 0$, the systems have no periodic orbits by the Bendixon criterion; see, for instance, [3, Thm. 7.10]. If $b = 0$, the systems are Hamiltonian, and then they have no limit cycles.

Now we bring together the local information previously obtained.

If $s \in (-2/\sqrt{3}, 2/\sqrt{3})$, the only equilibrium point is P_1, and if $b \neq 0$, it is always a node or a focus, stable or unstable. So, in any case, the phase portrait in the Poincaré disc is topologically equivalent to G1 in Figs. 2–3. If $b = 0$, then P_1 is a center, and the phase portrait in the Poincaré disc is topologically equivalent to G2 in Figs. 2–3.

If $s = |-2/\sqrt{3}|$, the equilibrium points are P_1 and P_2. If $b \neq 0$, the point P_2 is always a saddle-node, and P_1 is either a node or a focus, stable or unstable. In any of these cases, there is only one possible connection for the separatrices, and we obtain a phase portrait, which is topologically equivalent to G3 in Figs. 2–3. If $b = 0$, P_1 is a center, P_2 is a cusp, and the phase portrait is G4 in Figs. 2–3.

If $s \in \mathbb{R} \setminus (-2/\sqrt{3}, 2/\sqrt{3})$, there are three equilibria, P_1, P_3, and P_4. If $b \neq 0$, there is always one of the three equilibria, which is a saddle, and the other two equilibria are nodes or foci with the same stability. Then the phase portrait in the Poincaré disc is topologically equivalent to G5 in Figs. 2–3. If $b = 0$, then two of the equilibria are centers, and the other one is a saddle. So, there is only one possible connection for the separatrices, and the phase portrait is topologically equivalent to G6 in Figs. 2–3.

5 Proof of Theorem 3

We consider system (1) under conditions $b = -w = -3/\sqrt{22}$ and $k = -4/\sqrt{22}$, i.e.,

$$\dot{x} = y, \quad \dot{y} = x - x^3 - \frac{3}{\sqrt{22}}y + \frac{4}{\sqrt{22}}z, \qquad \dot{z} = \frac{3}{\sqrt{22}}(y - z). \tag{13}$$

These systems have the Darboux invariant

$$I_1 = \big(\sqrt{22}x^2 - \sqrt{22}x^4 - 4xy - 2\sqrt{22}y^2 + 16xz\big)\mathrm{e}^{4/\sqrt{22}t}.$$

Dynamics on the invariant surface

We restrict system (13) to $F_3 = (\sqrt{22}x^2 - \sqrt{22}x^4 - 4xy - 2\sqrt{22}y^2 + 16xz) = 0$ by setting $z = (-\sqrt{22}x^2 + \sqrt{22}x^4 + 4xy + 2\sqrt{22}y^2)/(16x)$, and we obtain the system

$$\dot{x} = y, \qquad \dot{y} = x - x^3 - \frac{3}{\sqrt{22}}y + \frac{-\sqrt{22}x^2 + \sqrt{22}x^4 + 4xy + 2\sqrt{22}y^2}{4\sqrt{22}x}. \tag{14}$$

Multiplying by x, we rescale time, and we get the system

$$\dot{x} = xy, \quad \dot{y} = \frac{3}{4}x^2 - \frac{3}{4}x^4 - \sqrt{\frac{2}{11}}xy + \frac{1}{2}y^2. \tag{15}$$

System (15) has three equilibrium points $(0,0)$, $(1,0)$, and $(-1,0)$. The eigenvalues of the Jacobian matrix at $(1,0)$ are $-\sqrt{2/1} \pm (4/\sqrt{11})\mathrm{i}$, and the eigenvalues of the Jacobian matrix at $(-1,0)$ are $1/\sqrt{22} \pm (4/\sqrt{11})\mathrm{i}$. Hence, $(1,0)$ is a hyperbolic stable focus, and $(-1,0)$ a hyperbolic unstable focus in system (15). Going back to system (14), both points, $(1,0)$ and $(-1,0)$, are stable foci.

The origin of system (15) is linearly zero, and we study it using the blow-up technique. As the direction $x = 0$ is characteristic, we first make a twist $(x, y) = (x_1 - y_1, y_1)$. In the new coordinates (x_1, y_1), system (15) becomes

$$\begin{aligned}
\dot{x}_1 &= \frac{3}{4}x_1^2 - \left(\frac{1}{2} + \sqrt{\frac{2}{11}}\right)x_1y_1 + \left(\frac{1}{4} + \sqrt{\frac{2}{11}}\right)y_1^2 - \frac{3}{4}x_1^4 + 3x_1^3y_1 \\
&\quad - \frac{9}{2}x_1^2y_1^2 + 3x_1y_1^3 - \frac{3}{4}y_1^4, \\
\dot{y}_1 &= \frac{3}{4}x_1^2 - \left(\frac{3}{2} + \sqrt{\frac{2}{11}}\right)x_1y_1 + \left(\frac{5}{4} + \sqrt{\frac{2}{11}}\right)y_1^2 - \frac{3}{4}x_1^4 + 3x_1^3y_1 \\
&\quad - \frac{9}{2}x_1^2y_1^2 + 3x_1y_1^3 - \frac{3}{4}y_1^4.
\end{aligned} \tag{16}$$

Now we perform the vertical blow-up $(x_1, y_1) = (x_1, x_1w_1)$, and system (16) becomes

$$\begin{aligned}
\dot{x}_1 &= \frac{3}{4}x_1^2 - \left(\frac{1}{2} + \sqrt{\frac{2}{11}}\right)x_1^2w_1 - \frac{3}{4}x_1^4 + \left(\frac{1}{4} + \sqrt{\frac{2}{11}}\right)x_1^2w_1^2 + 3x_1^4w_1 \\
&\quad - \frac{9}{2}x_1^4w_1^2 + 3x_1^4w_1^3 - \frac{3}{4}x_1^4w_1^4, \\
\dot{w}_1 &= \frac{3}{4}x_1 - \left(\frac{9}{4} + \sqrt{\frac{2}{11}}\right)x_1w_1 + \frac{3}{4}x_1^3 + \left(\frac{7}{4} + 2\sqrt{\frac{2}{11}}\right)x_1w_1^2 + \frac{15}{4}x_1^3w_1 \\
&\quad - \left(\frac{1}{4} + \sqrt{\frac{2}{11}}\right)x_1w_1^3 - \frac{15}{2}x_1^3w_1^2 + \frac{15}{2}x_1^3w_1^3 - \frac{15}{4}x_1^3w_1^4 + \frac{3}{4}x_1^3w_1^5.
\end{aligned} \tag{17}$$

Since x_1 is a common factor of $\dot{x}_1$ and $\dot{w}_1$, we rescale the time, and we get the differential system

$$\begin{aligned}
\dot{x}_1 &= \frac{3}{4}x_1 - \left(\frac{1}{2} + \sqrt{\frac{2}{11}}\right)x_1w_1 - \frac{3}{4}x_1^3 + \left(\frac{1}{4} + \sqrt{\frac{2}{11}}\right)x_1w_1^2 + 3x_1^3w_1 \\
&\quad - \frac{9}{2}x_1^3w_1^2 + 3x_1^3w_1^3 - \frac{3}{4}x_1^3w_1^4, \\
\dot{w}_1 &= \frac{3}{4} - \left(\frac{9}{4} + \sqrt{\frac{2}{11}}\right)w_1 + \frac{3}{4}x_1^2 + \left(\frac{7}{4} + 2\sqrt{\frac{2}{11}}\right)w_1^2 + \frac{15}{4}x_1^2w_1 \\
&\quad - \left(\frac{1}{4} + \sqrt{\frac{2}{11}}\right)w_1^3 - \frac{15}{2}x_1^2w_1^2 + \frac{15}{2}x_1^2w_1^3 - \frac{15}{4}x_1^2w_1^4 + \frac{3}{4}x_1^2w_1^5.
\end{aligned} \tag{18}$$

There are three equilibrium points on the straight line $x_1 = 0$: $(0, 1)$, which is a hyperbolic unstable node, and the two points $(0, (33+2\sqrt{22} \pm \sqrt{814})/(11+4\sqrt{22}))$, which are saddles. In Fig. 7(a), we include the local phase portrait of system (18) in a neighborhood of the straight line $x_1 = 0$. If we multiply by x to return to system (17), then all points on the x_1-axis become equilibrium points, and the orientation of the orbits in the second and third quadrants is reversed. Thus we obtain the phase portrait in Fig. 7(b) for system (17)

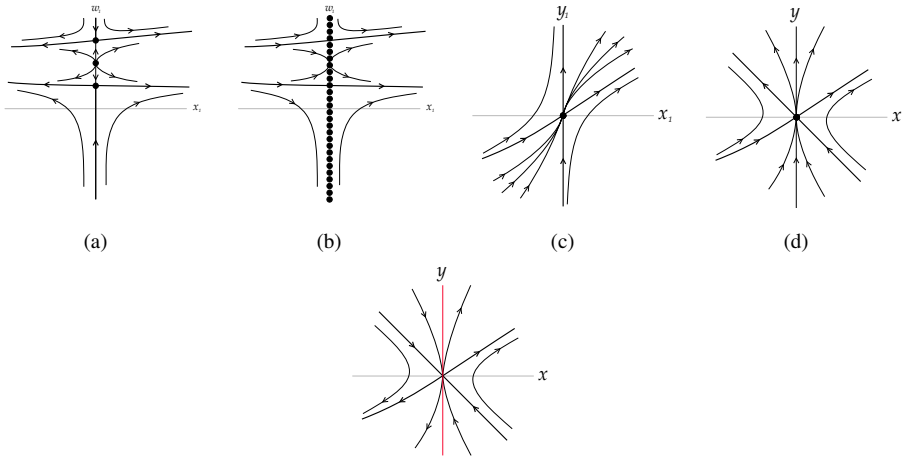

Figure 7. Blowing down of the origin of system (14).

around the straight line $x_1 = 0$. Now we undo the blow-up to obtain the local phase portrait at the origin of system (16), which is in Fig. 7(c). If we undo the twist, we obtain the local phase portrait at the origin of system (15), which is given in Fig. 7(d). Finally, if we undo the rescaling in the time variable, we obtain the local phase portrait for system (14), in which the vector field is not defined in $x_1 = 0$, and it is included in Fig. 7(e).

Now we study system (15) in the Poincaré disc. On the local chart U_1, system (15) is written as

$$\dot{u} = -\frac{3}{4} + \frac{3}{4}v^2 - \frac{\sqrt{22}}{11}uv^2 - \frac{1}{2}u^2v^2, \qquad \dot{v} = -uv^3.$$

Then there are no infinite equilibrium points in the local chart U_1.

On the local chart U_2, system (15) takes the form

$$\begin{aligned} \dot{u} &= \frac{1}{2}uv^2 + \frac{\sqrt{22}}{11}u^2v^2 + \frac{3}{4}u^5 - \frac{3}{4}u^3v^2, \\ \dot{v} &= -\frac{1}{2}v^3 + \sqrt{\frac{2}{11}}uv^3 + \frac{3}{4}u^4v - \frac{3}{4}u^4v - \frac{3}{4}u^2v^3. \end{aligned} \tag{19}$$

The origin is an equilibrium point, and it is linearly zero. So, we need to perform blow-ups to determine its local phase portrait. Since the vertical direction is characteristic, we need to make a twist $(u, v) = (u_1 - v_1, v_1)$. In the new coordinates (u_1, v_1), system (19) becomes

$$\begin{aligned} \dot{u}_1 &= \frac{1}{2}u_1v_1^2 - v_1^3 + \frac{\sqrt{22}}{11}u_1^2v_1^2 - \frac{\sqrt{22}}{11}u_1v_1^3 + \frac{3}{4}u_1^5 - 3u_1^4v_1 + \frac{15}{4}u_1^3v_1^2 - \frac{3}{2}u_1^2v_1^3, \\ \dot{v}_1 &= -\frac{1}{2}v_1^3 + \frac{\sqrt{22}}{11}u_1v_1^3 - \frac{\sqrt{22}}{11}v_1^4 + \frac{3}{4}u_1^4v_1 - 3u_1^3v_1^2 + \frac{15}{4}u_1^2v_1^2 - \frac{3}{2}u_1v_1^4. \end{aligned} \tag{20}$$

Now we perform the vertical blow-up $(u_1, v_1) = (u_2, u_2 v_2)$, and system (20) becomes

$$\begin{aligned}\dot{u}_2 &= \frac{3}{4}u_2^5 + \frac{1}{2}u_2^3 v_2^2 - 3u_2^5 v_2 \\ &\quad - \frac{\sqrt{22}}{11}u_2^4 v_2^2 - v_2^3 u_2^3 + \frac{15}{4}u_2^5 v_2^2 - \frac{\sqrt{22}}{11}u_2^4 v_2^3 - \frac{3}{2}u_2^5 v_2^3, \\ \dot{v}_2 &= -u_2^2 v_2^3 + u_2^2 v_2^4.\end{aligned} \tag{21}$$

Since u_2^2 is a common factor of $\dot{u}_2$ and $\dot{v}_2$, we rescale the time, and we get the differential system

$$\begin{aligned}\dot{u}_2 &= \frac{3}{4}u_2^3 + \frac{1}{2}u_2 v_2^2 - 3u_2^3 v_2 \\ &\quad - \frac{\sqrt{22}}{11}u_2^2 v_2^2 - v_2^3 u_2 + \frac{15}{4}u_2^2 v_2^2 - \frac{\sqrt{22}}{11}u_2^2 v_2^3 - \frac{3}{2}u_2^3 v_2^3, \\ \dot{v}_2 &= -v_2^3 + v_2^4.\end{aligned} \tag{22}$$

This system has on the straight line $u_2 = 0$ two equilibrium points: $(0, 1)$, which is a hyperbolic saddle, and $(0, 0)$, which is again linearly zero, so we continue performing vertical blow-ups. As the direction $x_2 = 0$ is characteristic, we make a twist $(u_2, v_2) = (u_3 - v_3, v_3)$. In the new coordinates (u_3, v_3), system (22) becomes

$$\begin{aligned}\dot{u}_3 &= \frac{3}{4}u_3^3 - \frac{9}{4}u_3^2 v_3 + \frac{11}{4}u_3 v_3 - \frac{9}{4}v_3^3 - 3u_3^3 v_3 + \left(9 + \frac{\sqrt{22}}{11}\right)u_3^2 v_3^2 \\ &\quad - \left(10 + \frac{2\sqrt{22}}{11}\right)u_3 v_3^3 + \left(5 + \frac{\sqrt{22}}{11}\right)v_3^4 + \frac{15}{4}u_3^3 v_3^2 \\ &\quad + \left(\frac{45}{4} - \frac{\sqrt{22}}{11}\right)u_3^2 v_3^3 + \left(\frac{45}{4} + \frac{2\sqrt{22}}{11}\right)u_3 v_3^4 \\ &\quad - \left(\frac{15}{4} + \frac{\sqrt{22}}{11}\right)v_3^5 - \frac{3}{2}u_3^3 v_3^3 - \frac{9}{2}u_3^2 v_3^4 - \frac{9}{2}u_3 v_3^5 + \frac{3}{2}v_3^6, \\ \dot{v}_3 &= -v_3^3 + v_3^4.\end{aligned} \tag{23}$$

Now we perform the vertical blow-up $(u_3, v_3) = (u_4, u_4 v_4)$, and system (23) becomes

$$\begin{aligned}\dot{u}_3\dot{u}_4 &= \frac{3}{4}u_4^3 - \frac{9}{4}u_4^3 v_4 - 3u_4^4 v_4 + \frac{11}{4}u_4^3 v_4^2 + \left(9 + \frac{\sqrt{22}}{11}\right)u_4^4 v_4^2 - \frac{9}{4}u_4^3 v_4^3 \\ &\quad + \frac{15}{4}u_4^5 v_4^2 - \left(10 + \frac{2\sqrt{22}}{11}\right)u_4^4 v_4^3 - \left(\frac{45}{4} + \frac{\sqrt{22}}{11}\right)u_4^5 v_4^3 \\ &\quad + \left(5 + \frac{\sqrt{22}}{11}\right)u_4^4 v_4^4 - \frac{3}{2}u_4^6 v_4^3 + \left(\frac{45}{4} + \frac{2\sqrt{22}}{11}\right)u_4^5 v_4^4 + \frac{9}{2}u_4^6 v_4^4 \\ &\quad - \left(\frac{15}{4} + \frac{\sqrt{22}}{11}\right)u_4^5 v_4^5 - \frac{9}{2}u_4^6 v_4^5 + \frac{3}{2}u_4^6 v_4^6,\end{aligned} \tag{24$_1$}$$

$$\begin{aligned}\dot{u}_3\dot{v}_4 = &-\frac{3}{4}u_4^2v_4 + \frac{9}{4}u_4^2v_4^2 + 3u_4^4v_4^2 - \frac{15}{4}u_4^2v_4^3 - \left(9+\sqrt{\frac{2}{11}}\right)u_4^3v_4^3 + \frac{9}{4}u_4^2v_4^4\\ &- \frac{15}{4}u_4^4v_4^3 + \left(11+2\sqrt{\frac{2}{11}}\right)u_4^3v_4^4 + \left(\frac{45}{4}+\sqrt{\frac{2}{11}}\right)u_4^4v_4^4\\ &- \left(5+\sqrt{\frac{2}{11}}\right)u_4^3v_4^5 + \frac{3}{2}u_4^5v_4^4 - \left(\frac{45}{4}+s\sqrt{\frac{2}{11}}\right)u_4^4v_4^5 - \frac{9}{2}u_4^5v_4^5\\ &+ \left(\frac{15}{4}+\sqrt{\frac{2}{11}}\right)u_4^4v_4^6 + \frac{9}{2}u_4^5v_4^6 - \frac{3}{2}u_4^5v_4^7. \qquad (24_2)\end{aligned}$$

Since u_4^2 is a common factor of $\dot{u}_4$ and $\dot{v}_4$, we rescale the time, and we get the differential system

$$\begin{aligned}\dot{u}_4 = &\frac{3}{4}u_4 - \frac{9}{4}u_4v_4 - 3u_4^2v_4 + \frac{11}{4}u_4v_4^2 + \left(9+\frac{\sqrt{22}}{11}\right)u_4^2v_4^2 - \frac{9}{4}u_4v_4^3\\ &+ \frac{15}{4}u_4^3v_4^2 - \left(10+\frac{2\sqrt{22}}{11}\right)u_4^2v_4^3 - \left(\frac{45}{4}+\frac{\sqrt{22}}{11}\right)u_4^5v_4^3\\ &+ \left(5+\frac{\sqrt{22}}{11}\right)u_4^4v_4^4 - \frac{3}{2}u_4^4v_4^3 + \left(\frac{45}{4}+\frac{2\sqrt{22}}{11}\right)u_4^3v_4^4\\ &+ \frac{9}{2}u_4^4v_4^4 - \left(\frac{15}{4}+\frac{\sqrt{22}}{11}\right)u_4^3v_4^5 - \frac{9}{2}u_4^4v_4^5 + \frac{3}{2}u_4^4v_4^6,\\ \dot{v}_4 = &-\frac{3}{4}v_4 + \frac{9}{4}v_4^2 + 3u_4^2v_4^2 - \frac{15}{4}v_4^3 - \left(9+\sqrt{\frac{2}{11}}\right)u_4v_4^3 + \frac{9}{4}v_4^4\\ &- \frac{15}{4}u_4^2v_4^3 + \left(11+2\sqrt{\frac{2}{11}}\right)u_4v_4^4 + \left(\frac{45}{4}+\sqrt{\frac{2}{11}}\right)u_4^2v_4^4\\ &- \left(5+\sqrt{\frac{2}{11}}\right)u_4v_4^5 + \frac{3}{2}u_4^3v_4^4 - \left(\frac{45}{4}+s\sqrt{\frac{2}{11}}\right)u_4^2v_4^5\\ &- \frac{9}{2}u_4^3v_4^5 + \left(\frac{15}{4}+\sqrt{\frac{2}{11}}\right)u_4^2v_4^6 + \frac{9}{2}u_4^3v_4^6 - \frac{3}{2}u_4^3v_4^7.\end{aligned} \qquad (25)$$

This system has on the straight line $u_4 = 0$ two equilibrium points, $(0,0)$ and $(0,1)$, which are both hyperbolic saddles.

Now we undo the blow-ups and twists. In Fig. 8(a), we plotted the local phase portrait of system (25) in a neighborhood of the straight line $u_2 = 0$. In Fig. 8(b), multiplying by u_4^2, we get the phase portrait of system (24). In Fig. 8(c), undoing the blow-up, we plotted the phase portrait at the origin of system (23). Undoing the twist, in Fig. 8(d), we plotted the phase portrait at the origin of system (22), and we included the phase portrait around the line $u_2 = 0$, adding the other equilibrium point, which was a saddle. Multiplying by u_2^2, in Fig. 8(e), we plotted the phase portrait around the straight line $u_2 = 0$ for system (21), and undoing the first blow-up, in Fig. 8(f), we plotted the local phase portrait around the straight line $u_2 = 0$ for system (20). Undoing the twist, we obtain the phase

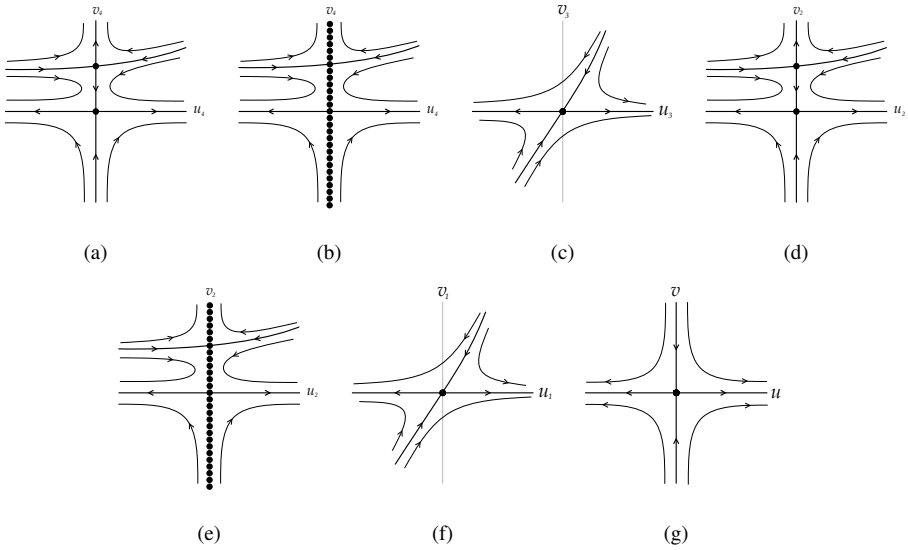

Figure 8. Blowing down of the origin of the chart U_2 of system (15).

portrait around the origin of the local chart U_2 for system (19), given in Fig. 8(g). For system (14), at infinity, we take into account that the system is not defined on the line $x = 0$ and that the orbits in the quadrants with $x < 0$ reverse their orientation.

Phase portraits in the Poincaré disc

Taking into account the local information obtained for the finite and infinite equilibrium points, now we study the local phase portrait in the Poincaré disc. We have two stable foci $(1, 0)$ and $(-1, 0)$; although the system is not defined on the straight line $x = 0$, in a neighborhood of the origin, we have the local phase portrait given in Fig. 7(e). The only infinite equilibrium points are the origins of the local charts U_2 and V_2, which have both two hyperbolic sectors. Then there are two possible configurations for the separatrices. The first one realizes when the unstable separatrix, which starts in a neighborhood of the origin, has its ω-limit in the stable focus on the positive x-axis; the stable separatrix, which ends in a neighborhood of the origin, has its α-limit in a neighborhood of the origin in the parabolic sector above the unstable separatrix, and in a symmetric way, in the quadrants with negative x. In this case, the global phase portrait is the one in Fig. 9(a). The other possibility corresponds with the case in which the two separatrices in the region $x > 0$ in the phase portrait in Fig. 7(e) are connected, i.e., there are actually the same separatrix; and the two separatrices in the region $x < 0$ are also connected. Then the orbits inside these regions delimited by the separatrices, which are homoclinic orbits, have their α-limit in those homoclinic orbits, and their ω-limits in the corresponding stable focus inside the region. The global phase portrait in this case is the one in Fig. 9(b). Numerically, using the software P4, we have obtained that the global phase portrait is the one in Fig. 9(a). The software P4 is a specialized computational tool designed for the numerical study of

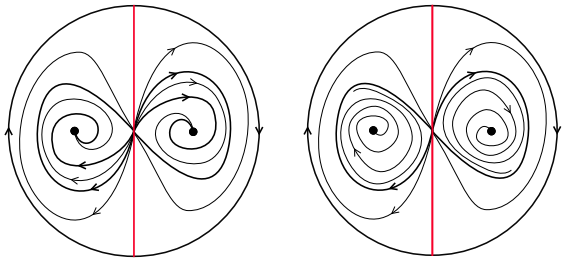

(a) (b)

Figure 9. Phase portraits of system (14) in the Poincaré disc.

planar polynomial vector fields. For more information about this software, see [3, Chap. 9] and [8].

α- and ω-limits

Here we want to determine the possible α- and ω-limits for the points in $\mathbb{R}^3$, which are not on the surface $F_3(x, y) = 0$ (as we have already determined, the phase portrait in this surface).

According to Proposition 6, as in this case $s = 4/\sqrt{22} > 0$, we have that for any $p = (x_0, y_0, z_0) \in \mathbb{R}^3$, $\omega(p)$ is contained in the closure $\overline{\{F_3(x, y, z) = 0\}}$ in the Poincaré ball. Also, we take into account that $\dot{x} = y$. Then, if $x_0, y_0 < 0$, the ω-limit of p is the point $(-1, 0, 0)$; if $x_0, y_0 > 0$, the ω-limit of p is the point $(1, 0, 0)$; if $x_0 y_0 < 0$, then the ω-limit of p is one of the following points: $(-1, 0, 0)$, $(1, 0, 0)$, $(0, 0, 0)$ or the endpoints of the y-axis.

Again, by Proposition 6, we know that $\alpha(p) \subset \overline{\{F_3(x, y, z) = 0\}} \cap \mathbb{S}^2$. Then, for the point p, the α-limit is the origin of the local chart U_2 or the origin of the local chart V_2, i.e., one of the endpoints of the y-axis.

6 Conclusions

In this work, we have studied the integrability and global dynamics of the autonomous Duffing–Holmes oscillator depending on the parameters b, k, and w.

We have studied the existence of invariant algebraic surfaces, obtaining a complete classification of all of those with degrees up to four. We have also studied all simple polynomial first integrals of the same degree. As a consequence, we have given parameter values for which the system is completely integrable.

Moreover, using the Poincaré compactification, we have described the global phase portraits of the systems, including the dynamics at infinity. We have described in detail the global dynamics in some relevant cases, including the reduction to planar systems when a first integral exists, and the detailed analysis of the dynamics on invariant algebraic surfaces associated with Darboux invariants. These results provide a rigorous description of the asymptotic behavior of the system.

The approach developed here can be applied to other polynomial vector fields of Duffing type or to higher-degree invariant surfaces, and may be useful in the analysis of integrability and global dynamics of related nonlinear oscillators arising in physics and applied sciences.

Author contributions. All authors (É.D-P., J.L., and M.V. O.-E.) have contributed in the methodology, formal analysis, software, validation, writing, review, and editing. All authors have read and approved the published version of the manuscript.

Conflicts of interest. The authors declare no conflicts of interest.

References

1. A. Cima, J. Llibre, Bounded polynomial vector fields, *Trans. Am. Math. Soc.*, **318**:557–579, 1990, https://doi.org/10.1090/S0002-9947-1990-0998352-5.
2. G. Donga, J. Llibre, Periodic orbits for an autonomous version of the Duffing–Holmes oscillator, *Nonlinear Anal. Model. Control*, **29**(6):1120–1126, 2024, https://doi.org/10.15388/namc.2024.29.37850.
3. F. Dumortier, J. Llibre, J.C. Artés, *Qualitative Theory of Planar Differential Systems*, Universitext, Springer, Berlin, Heidelberg, 2006, https://doi.org/10.1007/978-3-540-32902-2.
4. J. Llibre, M. Messias, R.P. da Silva, On the global dynamics of the Rabinovich system, *J. Phys. A, Math. Theor.*, **41**(27):275210, 2008, https://doi.org/10.1088/1751-8113/41/27/275210.
5. J. Llibre, R. Oliveira, Quadratic systems with an invariant conic having Darboux invariants, *Commun. Contemp. Math.*, **20**(4):1750033, 2018, https://doi.org/10.1142/S021919971750033X.
6. F. Sadyrbaev, I. Samuilik, From Duffing equation to bio-oscillations, in C.M.A. Pinto, C.M. Ionescu (Eds.), *Computational and Mathematical Models in Biology*, Nonlinear Syst. Complex., Vol. 38, Springer, Cham, 2023, pp. 159–182, https://doi.org/10.1007/978-3-031-42689-7.
7. A. Tamaševičius, S. Bumelienė, R. Kirvaitis, G. Mykolaitis, E. Tamaševičiūtė, E. Lindberg, Autonomous duffing–holmes type chaotic oscillator, *Elektron. Elektrotech.*, **93**(5):43–46, 2009, https://eejournal.ktu.lt/index.php/elt/article/view/10178.
8. Polynomial planar phase portraits – P4, https://mat.uab.cat/~artes/p4/p4.htm.